Earth and Planetary Science Letters 482 (2018) 367–376

Contents lists available at ScienceDirect

Earth and Planetary Science Letters

www.elsevier.com/locate/epsl

Ion microprobe $\delta^{18}O$ analyses to calibrate slow growth rate speleothem records with regional $\delta^{18}O$ records of precipitation

David Domínguez-Villar [a,*], Sonja Lojen [b,c], Kristina Krklec [d], Reinhard Kozdon [e,f], R. Lawrence Edwards [g], Hai Cheng [g,h]

[a] School of Geography, Earth and Environmental Sciences, University of Birmingham, Edgbaston, B15 2TT Birmingham, United Kingdom
[b] Department of Environmental Sciences, Jožef Stefan Institute, Jamova 39, SI-1000, Ljubljana, Slovenia
[c] Faculty of Environmental Sciences, University of Nova Gorica, Vipavska 13, 5000 Nova Gorica, Slovenia
[d] Department of Soil Science, Faculty of Agriculture, University of Zagreb, Svetošimunska 25, 10000 Zagreb, Croatia
[e] Lamont-Doherty Earth Observatory of Columbia University, 10964 Palisades (NY), USA
[f] Department of Geoscience, University of Wisconsin-Madison, 1215 West Dayton St., Madison 53706 (WI), USA
[g] Department of Earth Sciences, University of Minnesota, 55455 Minneapolis (MN), USA
[h] Institute of Global Environmental Changes, Xian Jiaotong University, 710049 Xian, China

ARTICLE INFO

Article history:
Received 19 July 2017
Received in revised form 14 October 2017
Accepted 4 November 2017
Available online xxxx
Editor: M. Frank

Keywords:
speleothem
paleoclimate
calibration
$\delta^{18}O$
ion microprobe
Postojna

ABSTRACT

Paleoclimate reconstructions based on speleothems require a robust interpretation of their proxies. Detailed transfer functions of external signals to the speleothem can be obtained using models supported by monitoring data. However, the transferred signal may not be stationary due to complexity of karst processes. Therefore, robust interpretations require the calibration of speleothem records with instrumental time series lasting no less than a decade. We present the calibration of a speleothem $\delta^{18}O$ record from Postojna Cave (Slovenia) with the regional record of $\delta^{18}O$ composition of precipitation during the last decades. Using local meteorological data and a regional $\delta^{18}O$ record of precipitation, we developed a model that reproduces the cave drip water $\delta^{18}O$ signal measured during a two-year period. The model suggests that the average water mixing and transit time in the studied aquifer is 11 months. Additionally, we used an ion microprobe to study the $\delta^{18}O$ record of the top 500 µm of a speleothem from the studied cave gallery. According to U–Th dates and ^{14}C analyses, the uppermost section of the speleothem was formed during the last decades. The $\delta^{18}O$ record of the top 500 µm of the speleothem has a significant correlation ($r^2 = 0.64$; p-value <0.001) with the modelled $\delta^{18}O$ record of cave drip water. Therefore, we confirm that the top 500 µm of the speleothem grew between the years 1984 and 2003 and that the speleothem accurately recorded the variability of the $\delta^{18}O$ values of regional precipitation filtered by the aquifer. We show that the recorded speleothem $\delta^{18}O$ signal is not seasonally biased and that the hydrological dynamics described during monitoring period were stationary during recent decades. This research demonstrates that speleothems with growth rates <50 µm/yr can also be used for calibration studies. Additionally, we show that the fit of measured and modelled proxy data can be used to achieve annually resolved chronologies in speleothems that were not actively growing at the time of collection and/or that do not record annual laminae.

1. Introduction

Speleothems can be excellent archives of paleoenvironment and/or paleoclimate (Fairchild and Baker, 2012), and the oxygen isotope composition of speleothems is the most commonly used proxy in speleothem records (e.g., Lauritzen and Lundberg, 1999; Wang et al., 2001; Domínguez-Villar et al., 2017). Most researchers interpret the variability of speleothem $\delta^{18}O$ records in relation to the variability of the inter-annual/long-term oxygen isotope composition of precipitation over the region. However, multiple controls affect the initial $\delta^{18}O$ value of precipitation once the water enters the karst system and before the isotopic composition of drip water is transferred to the speleothems (Baker et al., 2012). Detailed studies have proven that the $\delta^{18}O$ values of speleothems may be dominated by variability of the fractionation factor between the solution and the forming carbonate (Feng et al., 2014). The epikarst hydrology has a significant control on

* Corresponding author.
E-mail address: ddvillar@hotmail.com (D. Domínguez-Villar).

https://doi.org/10.1016/j.epsl.2017.11.012
0012-821X/

the $\delta^{18}O$ values due to the mixing of groundwater reservoirs with different residence times (Bradley et al., 2010). Also, the interactive dynamics between the soil and the atmosphere can affect the isotope composition via groundwater evaporation (Ayalon et al., 1998; Markowska et al., 2016) or the thermal decoupling between ground and atmosphere temperature (Domínguez-Villar et al., 2013). Therefore, before conducting detailed paleoenvironmental and/or paleoclimate interpretations from speleothem records, it is desirable to evaluate whether such records can be calibrated with available geochemical, environmental or climatological time series that control the $\delta^{18}O$ values in the system. Previous studies have shown a lack of correlation or a non-stationary relationship between Holocene speleothem $\delta^{18}O$ records and climate variables due to the complexity on the controls affecting the $\delta^{18}O$ values in karst systems (Treble et al., 2005; Fischer and Treble, 2008; Baker et al., 2011). Therefore, it is a good practice to perform calibration tests covering a period lasting no less than a decade in order to conduct robust paleoclimate or paleoenvironmental reconstructions (Burns et al., 2002; Yudava et al., 2004; Jex et al., 2010; Riechelmann et al., 2017).

In order to perform accurate calibration tests, annually resolved chronologies and annual or sub-annual sampling resolutions of the studied proxy are required (e.g., Mattey et al., 2008). Since growth rate is a limiting factor for these studies, speleothems used to calibrate $\delta^{18}O$ records typically have growth rates in the order of several hundred of microns per year. The amount of sample required to perform $\delta^{18}O$ analyses by Gas Source Isotope Ratio Mass Spectrometry (GS-IRMS) limits the spatial sampling resolution along the growth rate of speleothems to a range between 50 and 100 µm in best scenarios (Spötl and Mattey, 2006; Pacton et al., 2013). However, $\delta^{18}O$ analyses can also be carried out using an ion microprobe, which smaller requirements for sample size allows a typical spatial resolution between 10 and 30 µm (Treble et al., 2007; Orland et al., 2009). The use of ion microprobes to study speleothems is not novel, although is still uncommon. This technology has been applied to speleothems to obtain high resolution $\delta^{18}O$ records (Kolodny et al., 2003; Treble et al., 2007), to unravel seasonal cycles (Liu et al., 2015), to study the paleo-seasonality (Orland et al., 2009, 2012, 2015) or to perform calibration of recent samples (Treble et al., 2005; Orland et al., 2014). These studies showed that the spatial resolution of the ion microprobe analyses represents an advantage compared to the combination of micromill sampling and GS-IRMS analyses.

During two years we monitored the water $\delta^{18}O$ values of several drip sites in a hall of Postojna Cave (Slovenia) and selected a laminated speleothem that grew under one of the studied drip sites. Due to the slow growth rate of the top 30 mm of the speleothem (<40 µm/yr), we used ion microprobe analyses to obtain a speleothem $\delta^{18}O$ record of the top 500 µm of the sample that was expected to precipitate over the last decades. The aim of the study is to compare the recent speleothem $\delta^{18}O$ record with the regional record of $\delta^{18}O$ values of precipitation to test whether this speleothem record will provide a robust proxy for the long-term evolution of the $\delta^{18}O$ values of precipitation in the region.

2. Material and methods

2.1. Postojna Cave and water analyses

Postojna Cave is a 20 km long tourist cave in Slovenia (45.78°N; 14.20°E) (Fig. 1A). Within this cave, Pisani Rov is a ~0.6 km long corridor aside from the major tourist route. We focus our study on Bela in Rdeča hall (hereafter referred to as BiR hall), which is the last chamber at the far end of Pisani Rov (Fig. 1B). BiR hall is 70 m long, 12 m wide and has an average height of 4.5 m. This hall has

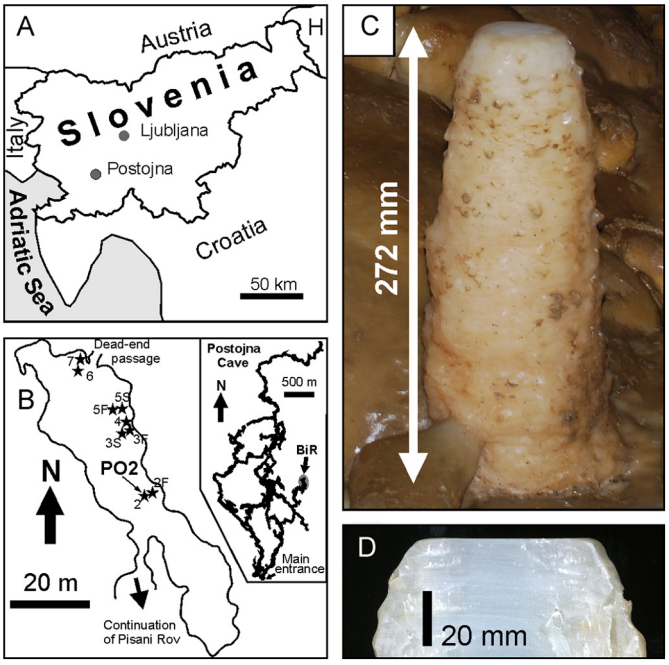

Fig. 1. Location map, cave sketch and speleothem images. A: Location map of Slovenia. Records of $\delta^{18}O$ values of precipitation are from Ljubljana and Postojna. The studied cave is in Postojna. B: Sketch of BiR hall (plan view) showing the location of drip sites (stars). Studied speleothem (PO2) was collected from drip site 2. Inset graph shows the location of BiR hall within Postojna Cave (grey shaded area pointed with an arrow). C: Image of stalagmite PO2 before collection. D: Detailed image of the top 30 mm of PO2 speleothem showing the flat surface of the centre of the speleothem.

nearly 40 m of bedrock cover. The room is decorated with a multitude of speleothems, it has no appreciable air flow, and its average temperature is 8.4 °C (Domínguez-Villar et al., 2015). The surface over the cave has a patchy distribution of rendzina soils in between the dominant bedrock exposures that stands <0.5 m from the ground. According to artificial pits, the soil can locally reach depths >0.5 m (Krajnc et al., 2017). The vegetation consists of a dense mixed forest (i.e., spruce, fir and beech trees). In the studied site the climate is continental, and based on data from the Postojna meteorological station, located at 533 m asl (above sea level), the mean annual temperature was 8.7 °C during the period 1971–2000, with a mean temperature of 18.1 °C during the warmest month (July) and 0.1 °C during the coldest month (January). Over the same period, the average amount of annual precipitation (±1 SD; standard deviation) was 1590 ± 209 mm. There is no clear seasonality in the amount of precipitation. Snow is common during the winter and the snow cover over the ground can last for weeks during these months.

During a two-year period (2009–2010), we studied the isotope composition of 9 drip sites in BiR hall, all of them located within 40 m (Fig. 1B). Drip water samples were collected twice per month for analyses of $\delta^{18}O$ values. These samples consisted of water accumulated in beakers left under the drip sites since the previous visit, except for one site (site 7; Fig. 1B) that had enough discharge to collect the water during every cave visit. Additionally, a total of 15 beakers containing 50 ml of water with a known initial $\delta^{18}O$ value (+19.16‰ VSMOW) were left to equilibrate with the moisture of the cave atmosphere in BiR gallery to evaluate potential evaporation processes. These samples were all set at once and collected one by one in different visits to the cave. The samples were set under an umbrella to prevent interferences caused by splashing water from nearby drip sites. Water samples of monthly precipitation were collected at the meteorological station of Postojna. All precipitation, rainfall, snow or hail, was collected daily and trans-

ferred to a larger bottle that was replaced every month. The bottles were tightly caped to prevent evaporation and kept in a cool and dark place until their transport to the laboratory. The $\delta^{18}O$ values of water samples were determined by equilibration with CO_2 for 12 h at 25 °C (Epstein and Mayeda, 1953). The analyses were conducted in an IsoPrime continuous flow GS-IRMS with Multiflow Bio equilibration unit at Jožef Stefan Institute (Slovenia). Measurements were calibrated with two working standards (MiliQ water and snow, calibrated versus VSMOW2 and VSLAP2) and USGS47, USGS48 and USGS49 reference materials were used as controls. Results are reported as ‰ VSMOW and the uncertainty of these measurements is ±0.1‰. A stalagmite was collected from one of the studied drip sites (drip site 2; Fig. 1B, 1C). An acoustic drip rate counter from Driptych (Stalagmate) was installed at this drip site to study the discharge dynamics. The drip rate was recorded at intervals of 10 min and integrated into daily drop counts.

2.2. Preparation and analyses of the speleothem

The collected speleothem (PO2) is a 272 mm long stalagmite (Fig. 1C). The speleothem was halved along the longitudinal axis and a polished slab was obtained from the central section of the sample. In order to estimate the growth rate of the top of the sample, we calculated U–Th dates from the topmost 30 mm of the stalagmite. We used a hand drill with a 0.9 mm drill bit to obtain 200 to 300 mg of speleothem sample at different distances from the top of the stalagmite following the laminae structure. Sample digestion, spiking and U and Th separation followed a standard procedure (Edwards et al., 1986; Dorale et al., 2004). U and Th isotopes were measured with a NEPTUNE multi collector inductively coupled plasma mass spectrometer at the Department of Geosciences of the University of Minnesota. Ages were calculated according to updated decay constants (Cheng et al., 2013) and assuming an initial $^{230}Th/^{232}Th$ atomic ratio of $4.4 \pm 2.2 \times 10^6$. The reported age uncertainty considers 2 SD of the isotope ratios and its propagation through calculations. Growth rate was calculated using Bayesian statistics by implementing these dates and their uncertainties in the software Oxcal (Ramsey, 2008). We used a P-sequence model of setting "K0" parameter to 0.01 mm^{-1} with a dynamic range from 10^{-2} to 10^2. Radiocarbon analyses were performed to estimate the ^{14}C activity of the top 2 mm of the speleothem. A hand drill equipped with a 0.3 mm drill bit was used to collect 10 to 30 mg of carbonate. A sample of Icelandic spar was collected using the sample protocol and used as a background sample. Analyses were carried out at the SUERC AMS Laboratory. Results are provided as proportion of modern carbon (pMC) and 1 SD was considered for the calculation of the uncertainties. The central part of PO2 stalagmite has thin visible laminae, keeping a very similar structure throughout the speleothem. We prepared a polished rock section 400 µm thick mounted on a glass plate in order to observe the laminae under optical microscope. From this rock section, we cut a smaller section (3.5 mm wide and 6 mm long) that covers the top of the stalagmite. This small piece of rock section was used to prepare a mount for ion microprobe analyses and to obtain more detailed images of the laminae using a confocal laser fluorescence microscope (CLFM). This mount is an epoxy disc 1-inch in diameter that contains the small portion of the rock section and two grains of UWC-3 (calcite standard; $\delta^{18}O = +12.49$‰ VSMOW; Kozdon et al., 2009). The section of the speleothem and the standard materials to be analysed by the ion microprobe were arranged within 5 mm of the centre of the mount in order to prevent analytical bias related to the sample position (Valley and Kita, 2005; Kita et al., 2009). The surface of the mount was smoothed and polished using a final polishing solution of colloidal alumina (0.05 µm). Optical microscope and a scanning electron microscope (SEM) were used to check the quality of the polished surface to be sure that sample topography was not larger than 5 µm.

Prior to ion microprobe analyses, the sample mount was cleaned with ethanol and deionised water, dried and subsequently coated with a ~60 nm thick film of gold. In situ analyses of $\delta^{18}O$ were carried out using the WiscSIMS CAMECA ims-1280 large radius multicollector ion microprobe at the University of Wisconsin-Madison. We used a ~1.7 nA primary beam of $^{133}Cs^+$ ions, focused to a ~13 µm beam spot at the surface of the sample. The resulting analysis pits were ~1 µm deep and covered a nearly circular ellipse area which minor axis, oriented parallel to the growth axis of the speleothem, was ~13 µm long. Charging of the sample was compensated by an electron flood gun in combination with the gold coating of the mount. Before and after each speleothem sample batch, 4 samples of the UWC-3 standard were analysed to calculate the $\delta^{18}O$ value of individual speleothem analysis. Each batch of speleothem analyses was limited to a maximum of 15 samples. The reproducibility of individual spot analyses of UWC-3 standard carried out before and after each batch of speleothem analyses was assigned as the uncertainty of those speleothem analyses. The average uncertainty of $\delta^{18}O$ analyses during the analytical session was ±0.34‰ (2 SD).

Images of fluorescent laminae were obtained after ion microprobe analyses were completed using a Nikon Air Multi-Photon CLFM at the University Image Center of the University of Minnesota, operating with a 488 nm argon-sourced laser line. The images were filtered for wavelengths between 505 and 539 nm. Using these images, laminae were counted in different sectors of the sample to evaluate whether they have an annual periodicity supported by the independent chronological information provided by the U–Th dates.

3. Results

3.1. Cave monitoring

The nine records showing the water $\delta^{18}O$ values of the monitored cave drip sites show a relatively homogeneous variability during the studied period (Fig. 2A). The maximum amplitude of the average record is <1‰. There is no seasonal pattern in any of the $\delta^{18}O$ time series and most of the recorded amplitude results from a 5 month period in the first half of the year 2010, when $\delta^{18}O$ values were on average 0.5‰ more negative than during the rest of the record. The water samples left to equilibrate with the moisture of the cave atmosphere showed no sign of volume loss due to evaporation, confirming that relative humidity was ~100% through the year. The $\delta^{18}O$ values of these samples took 3 months to equilibrate with the moisture of the cave atmosphere (i.e., the isotope values of the water samples stopped shifting from the original isotope composition and started having a normal variability around a mean). The average isotope composition of these equilibrated waters is within 0.2‰ of most of the studied drip sites during the same period. Collection of water samples for $\delta^{18}O$ analyses of precipitation on the meteorological station of Postojna started at the onset of the year 2009. The record of $\delta^{18}O$ values of precipitation has a strong seasonality (Fig. 2B) and the annual weighed average $\delta^{18}O$ value of precipitation for the years 2009 and 2010 was −8.4 and −8.3‰ VSMOW respectively.

Drip rate that fed the stalagmite PO2 (drip site 2) was studied for over two years. The record shows a complex pattern (Fig. 3), characteristic of drip sites fed by more than one reservoir (Bradley et al., 2010). The drip rate had a characteristic background level of less than 10 drops per day. This pattern was disrupted after certain precipitation events that caused an exponential increase in the drip rate. The sudden change in drip rate after precipitation occurred generally within the same day and rarely exceeded

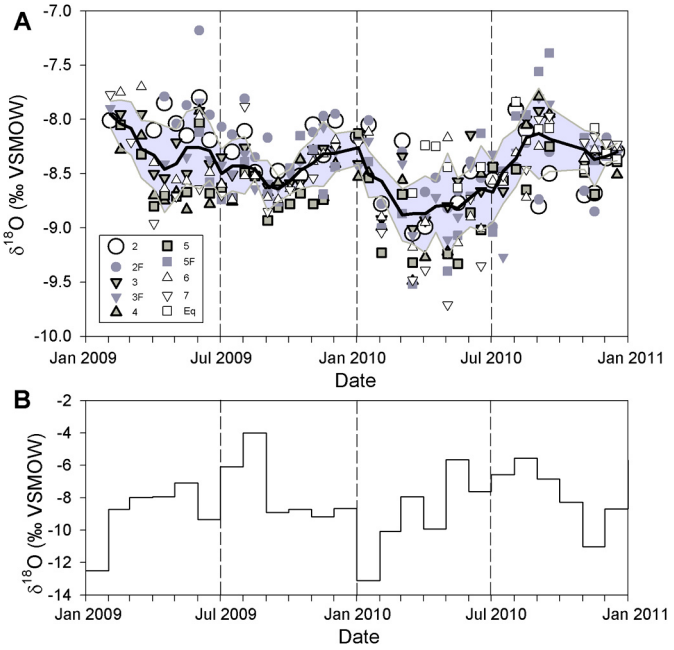

Fig. 2. Records of $\delta^{18}O$ values of BiR drip water and Postojna precipitation during the years 2009 and 2010. A: Water $\delta^{18}O$ values of 9 drip sites of BiR hall. Grey shaded area shows the range between the upper and lower boundary of the 1 standard deviation of the 9 drip site records for every observational period, plotted from their average $\delta^{18}O$ value. The record of water equilibrated with the moisture of the cave atmosphere (eq) is also shown. B: Monthly record of Postojna $\delta^{18}O$ values of precipitation.

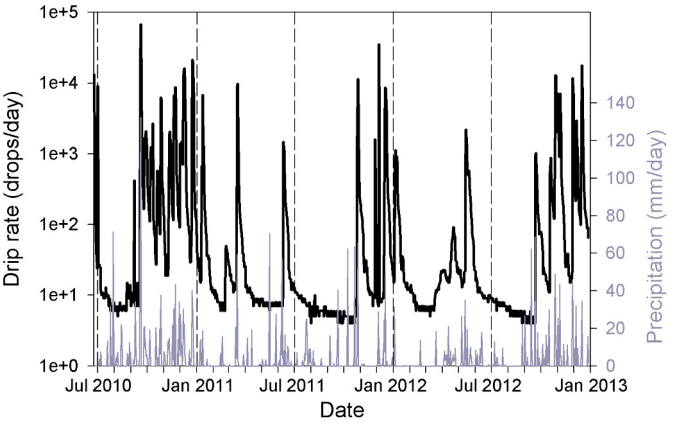

Fig. 3. Records of drip rate at site 2 and amount of precipitation measured at Postojna meteorological station.

more than 2 days of delay. However, not all precipitation events resulted in a drip rate increase. During autumn and winter, drip rate responded more often to external precipitation events, preventing the drip rate to reach its background level of drip rate. Therefore, autumn and winter months had generally higher drip rates compared to those of spring and summer months.

3.2. Chronology of PO2 top stalagmite

Based on the age model of PO2 stalagmite, that uses five U–Th dates collected between 5 and 28 mm from the top of the speleothem (Table S1 in Supplementary Material), the average growth rate along that section oscillates between 15 and 40 µm/yr (Fig. 4). This age model shows that the top 30 mm of the speleothem grew for more than one millennium since ~1200 yr BP until recent times. Additionally, the ^{14}C activity of three samples collected from the topmost 2 mm of the speleothem was analysed. Results show that the ^{14}C activity of the topmost sample has a value >100 pMC, whereas the other two samples record values <95 pMC (Table S2 in Supplementary Material). Speleothem values of ^{14}C activity above 100 pMC are expected for calcite precipitated after 1960s due to nuclear bomb tests (Genty et al., 1998; Vokal, 1999; Genty and Masault, 1999). This supports that the section of the topmost 0.5 mm of the speleothem precipitated during the last decades. However, we have not observed precipitation of any calcite on the artificial substrates deployed under drip site 2 during the years of cave monitoring.

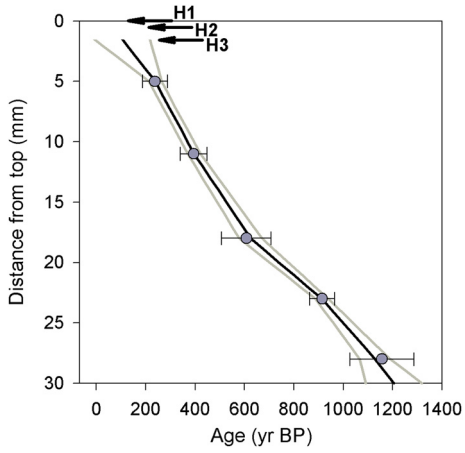

Fig. 4. Age model of PO2 speleothem between 1.4 and 30 mm from the top of the sample (black line). Grey lines represent the uncertainty of the age model. H1, H2 and H3 are three hiati identified at 0, 0.5 and 1.4 mm from the top of the sample. Grey dots and error bars are the U–Th dates and their uncertainties.

The top of PO2 speleothem is a flat surface with a ~50 mm diameter in the centre/axial part of the speleothem. Laminae in the central sector of the speleothem mostly adapt to such flat morphology. The structure of the laminae is very similar along the 272 mm of the speleothem. However, in the top 1.4 mm of the sample we observe three anomalous dark surfaces at 0, 0.5 and 1.4 mm from the top (Fig. 5A). Lateral continuity of laminae is occasionally disrupted by these surfaces, especially along small vertical pits (generally <2 mm in depth) showing dissolution of calcite along these surfaces (see Supplementary Material). Therefore, we identify them as hiati, and starting from the top, we name them H1, H2 and H3 (Fig. 4, Fig. 5). The small dissolution features observed at the top of the speleothem suggest that the sample was not growing at the time of collection. These observations are in agreement with the lack of calcite precipitated during the monitoring period in artificial substrates at this site. According to the U–Th age model, these three hiati occurred within the last 200 yr. Therefore, during this period, variable cave environmental conditions favoured either the PO2 speleothem growth or the formation of hiati.

PO2 speleothem contains laminae through the sample that could be used to improve the chronology. Each lamina consists of a couplet of clear and dark calcite layers under optical microscope and a couplet of more and less fluorescent layers under fluorescence microscope. We count and measure the thickness of laminae from the fluorescence image due to their clearer definition. The thickness of fluorescent laminae range from 2 to 27 µm, and the average thickness is 6 µm (Table S3 in Supplementary Material). The structure and the average thickness of laminae below H3 hiatus do not differ from those above it. The average vertical thickness of speleothem growth per year (growth rate) calculated based on U–Th dates is ~5 times larger than the measured thickness of laminae. Additionally, we identified 81 laminae between H1 and H2 hiati, and 148 laminae between H2 and H3 hiati. The time lapsed since the last deposited calcite recorded before H3 hiatus to the

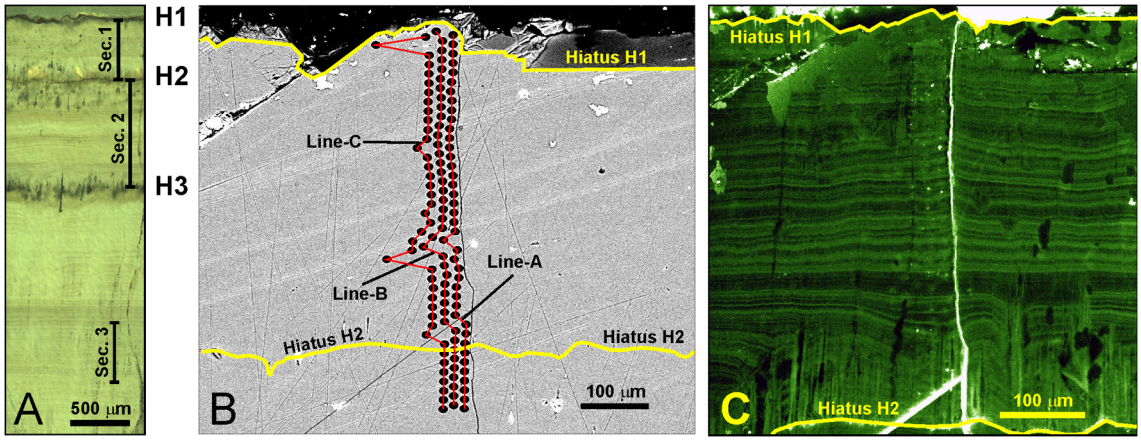

Fig. 5. Microscope imaging of PO2 speleothem. A: Optical microscope image of top 3.5 mm of PO2 speleothem. Three hiati (H1, H2 and H3) are clearly visible. Vertical capped lines identify the three sections were laminae were counted (see Table S4 in Supplementary Material). B: Scanning electron microscope image showing the ion microprobe sampling routine along 3 different lines. Black ellipses show the dimension of every analytical spot. Yellow lines are hiati surfaces. Hiatus H1 is at the top of the speleothem regardless the false impression of the image due to different focal planes. C: Confocal laser fluorescence microscope image of the top 500 μm of PO2 speleothem showing fluorescent laminae. The thickness of fluorescent laminae is thinner than the size of the analytical spots of the ion microprobe analyses, preventing the study of intra-laminae $\delta^{18}O$ variability. White lines are cracks, whereas black areas represent material without fluorescence. The patchy sections with fluorescence patterns disrupting the laminae are the result of areas where the gold coat was not properly removed before imaging. (For interpretation of the references to colour in this figure legend, the reader is referred to the web version of this article.)

moment of speleothem collection can be estimated considering the most recent U–Th date and its uncertainty, the distance between the position where the U–Th sample was collected and the H3 hiatus, and the average growth rate of the sample. Assuming a limited change in growth rate is reasonable as confirmed by the same average thickness of laminae above and below the hiati. Thus, it is estimated that 164 ± 51 yr passed since the last deposition of calcite recorded below the H3 hiatus and the time of speleothem collection. Above H3 hiatus we counted 229 laminae, a number substantially larger than the expected numbers of years until the sample collection. Additionally, this comparison does not consider the duration of the three hiati that would decrease the duration of the available period for the formation of laminae. These evidence confirm that laminae from PO2 stalagmite do not have an annual periodicity and cannot be used to improve the speleothem chronology.

3.3. *Speleothem ion microprobe $\delta^{18}O$ analysis*

We analysed the $\delta^{18}O$ record of 0.6 mm along the top of PO2 speleothem in situ by ion microprobe. The series of individual analyses were arranged following three parallel lines/transects (A, B and C) oriented perpendicular to the top of the speleothem. Analytical spots are 15 μm apart along the lines to avoid overlapping of the analytical pits. The parallel lines of analyses are only 18 μm apart, and line B analyses are 7.5 μm displaced along the line to provide a dense packing of analyses and avoid the nearly overlap of analytical spots of the different lines (Fig. 5B). When cracks or other defects on the polished surface occurred along the lines, the location of the analysis was adjusted laterally, keeping the same distance to the top. The analyses were also conducted below the second hiatus (H2) to test if there is any significant variability across the discontinuity, although the focus of these analyses is to establish a calcite $\delta^{18}O$ record at the top of the stalagmite between hiati H1 and H2.

The results show that the $\delta^{18}O$ variability along the studied lines is within 3‰ and the average value is −6.33‰ (Fig. 6; Table S4 in Supplementary Material). Before and after the H2 hiatus, the analyses show similar $\delta^{18}O$ values and variability. The records along the three lines nicely replicate each other within analytical uncertainty. Therefore, we integrate the results of the three lines in a composite $\delta^{18}O$ record by averaging the values of the three

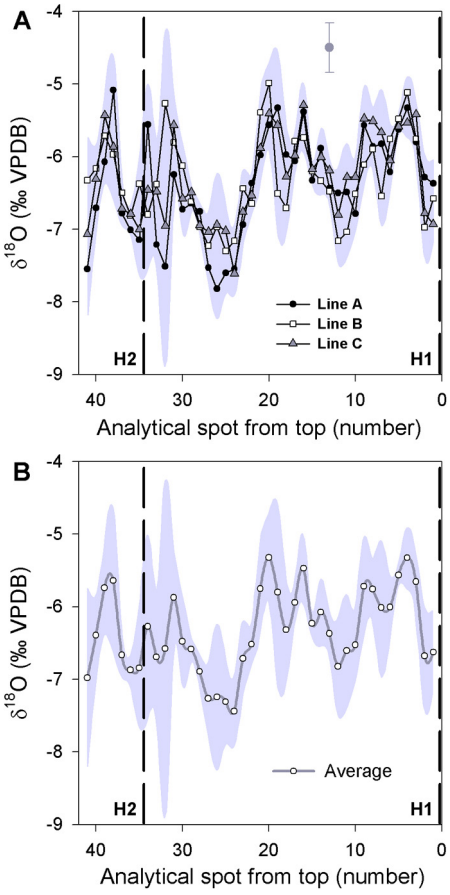

Fig. 6. Ion microprobe $\delta^{18}O$ analyses of the top 600 μm of PO2 speleothem. A. Speleothem $\delta^{18}O$ records along the tree parallel lines. The location of hiati H1 and H2 are represented by the black vertical dashed lines. The grey dot with error bars represents the average uncertainty of ion microprobe analyses. Grey shaded area shows the range between the upper and lower boundaries of the 2 standard deviations of the 3 samples at similar distance from the top of the speleothem along the 3 parallel sampling lines, plotted from their average $\delta^{18}O$ value. B. Average $\delta^{18}O$ record of PO2 speleothem used for calibration. The grey shaded area and hiati lines are the same shown in A.

analytical spots with similar distance to the top of the speleothem (triplets). The ±2 SD envelope of the triplets along the record contains all analyses, and still, the $\delta^{18}O$ variability of the record is larger than this envelope, enabling further study of the isotope variability of the sample. The composite record integrates small lateral and vertical variations of the $\delta^{18}O$ values of calcite, an assumable simplification since the results are still within the analytical uncertainty of the analyses. We used this composite $\delta^{18}O$ record in further calculations of the calibration test.

4. Discussion

4.1. Regional record of $\delta^{18}O$ values of precipitation

PO2 stalagmite was not actively growing at the time of collection and consequently we cannot use the record of $\delta^{18}O$ values of precipitation over Postojna Cave to calibrate our speleothem record. The nearest record of $\delta^{18}O$ values of precipitation is from Ljubljana (46.07°N; 14.52°E; 299 m asl), located only 40 km northeast of Postojna (Fig. 1A). The available record of $\delta^{18}O$ values of precipitation from Ljubljana covers the period from 1981 to 2010 (IAEA/WMO, 2009). During the years 2009 and 2010 we have monthly $\delta^{18}O$ values from Postojna and Ljubljana and their $\delta^{18}O$ records have a significant correlation ($r^2 = 0.66$; p-value <0.001). The average of the monthly $\delta^{18}O$ values of precipitation is 0.56‰ more negative in Ljubljana than in Postojna. The climate in Postojna and Ljubljana, that is expected to control the $\delta^{18}O$ values of precipitation, is very similar. During the years 2009 and 2010 the monthly temperature records of both locations have a strong correlation ($r^2 = 0.99$; p-value <0.001), being Postojna in average 1.5 °C warmer than Ljubljana. The correlation of temperature records and the thermal difference between both sites were stable during the full available instrumental record (Domínguez-Villar et al., 2015). The amount of precipitation recorded in both locations is also correlated ($r^2 = 0.50$; p-value < 0.001), with Ljubljana having 15% less precipitation than Postojna. However, amount of precipitation is not a significant control of the $\delta^{18}O$ values of precipitation neither in Ljubljana (Vreča et al., 2006) nor in Postojna. Thus, considering an isotope gradient in relation to temperature of 0.30‰/°C, the average difference in the monthly $\delta^{18}O$ values of precipitation between both locations is mostly explained by the cooler temperature recorded in Ljubljana (i.e., based on the temperature control alone, $\delta^{18}O$ values of precipitation in Ljubljana are expected to be on average 0.45 ± 0.01‰ more negative than in Postojna). Therefore, although other controls could also contribute to the $\delta^{18}O$ values of precipitation in these two sites, it is clear that temperature is a major control of its variability and explains most of the observed differences in the $\delta^{18}O$ values. The good correlation of $\delta^{18}O$ values of precipitation and its main known control (i.e., temperature) between both locations support the use of Ljubljana $\delta^{18}O$ record as a good indicator of the $\delta^{18}O$ values of precipitation over Postojna cave. The complete record of monthly $\delta^{18}O$ values of precipitation at Ljubljana from 1981 to 2010 and $\delta^{18}O$ weighed annual record are provided in Fig. 7.

The detailed interpretation of the $\delta^{18}O$ values of precipitation in terms of climate is still under investigation since in addition to temperature, other parameters could explain part of the observed variability. Thus, some authors using weather types have suggested that the source of precipitation could contribute to the $\delta^{18}O$ values of Ljubljana (Brenčič et al., 2015). On the other hand, a preliminary study based on back trajectory analyses and hydro-meteorological models supports that moisture sources have a negligible impact on the $\delta^{18}O$ values over Postojna (Krklec et al., 2016). The discrepancy between these studies confirms the complexity of understanding in depth the climate controls on the $\delta^{18}O$ values of precipitation, a topic beyond the scope of the present study.

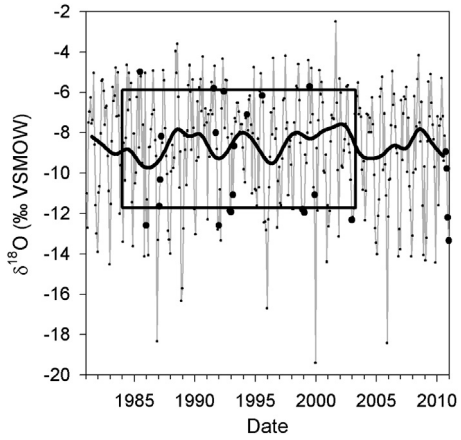

Fig. 7. Record of monthly $\delta^{18}O$ values of precipitation from Ljubljana. The record of annual weighed isotope values is represented as a black bold line. The rectangle highlights the period between the years 1984 and 2002 (both included). Larger circles represent reconstructed $\delta^{18}O$ values missing in the original dataset. Missing data from the Ljubljana $\delta^{18}O$ record ($n = 23$) were calculated assuming temperature as a main control of the $\delta^{18}O$ values of precipitation and considering data within the 95% confidence interval. The resulting equation is: $\delta^{18}O = -12.105 + (0.302 \cdot T)$, where T is the temperature in Ljubljana measured in °C at 2 m elevation ($r^2 = 0.83$, p-value < 0.001).

4.2. The role of karst hydrology in the transfer of the $\delta^{18}O$ signal

During the two years of monitoring program, the $\delta^{18}O$ signal of the water from studied drip sites showed no seasonality. This is in agreement with a previous study conducted during a year in the same gallery that analysed water from two drip sites and one pool at a monthly interval (Vokal, 1999). These results imply that the clear seasonality of the $\delta^{18}O$ values of precipitation was filtered out during the transfer of the infiltrated water to BiR hall. However, the drip water $\delta^{18}O$ time series record substantial variability during the monitoring period. All drip sites showed a similar trend of $\delta^{18}O$ values, and the amplitude of the average $\delta^{18}O$ time series considering all drips is 0.9‰. Thus, the particular mixing dynamics of percolated water along different routes to each drip site does not modify the $\delta^{18}O$ signal enough to blur the variability provided by the isotope composition of the infiltrating water. Therefore, we have developed a model that provides the average $\delta^{18}O$ values of drip sites in BiR hall.

Monthly $\delta^{18}O$ values of precipitation from Postojna were reconstructed back to 1981 using the Ljubljana $\delta^{18}O$ record based on their correlation during the years 2009 and 2010. The model used data from Postojna meteorological station between 1980 and 2010 and considers evapotranspiration in the system, as well as accounts for infiltration delays related to existing snow cover at the end of the month. Details of the model are provided in Supplementary Material. The output of the model calculates $\delta^{18}O$ values of drip water that are within the ±2 SD envelope around the average measured drip water $\delta^{18}O$ values (Fig. 8). The best fit of our model to the averaged record of measured drip water $\delta^{18}O$ values supports a mixing period and transit time in the epikarst of 11 months ($r^2 = 0.63$; p-value <0.001) since the moment of infiltration until the water drips in BiR hall. The correlation of the model is still significant (with p-values <0.005) at 10 and 12 months, although with lower correlation coefficients ($r^2 = 0.43$ and 0.36 respectively).

Our results show that PO2 speleothem has fluorescent laminae. Fluorescence in speleothems is related to organic matter derived from the soil that is flushed into the epikarst before being entrapped in the speleothem (e.g., Baker et al., 1996). A positive relationship has been reported between dissolved organic matter and discharge (Ban et al., 2005). The record of drip rate from drip site

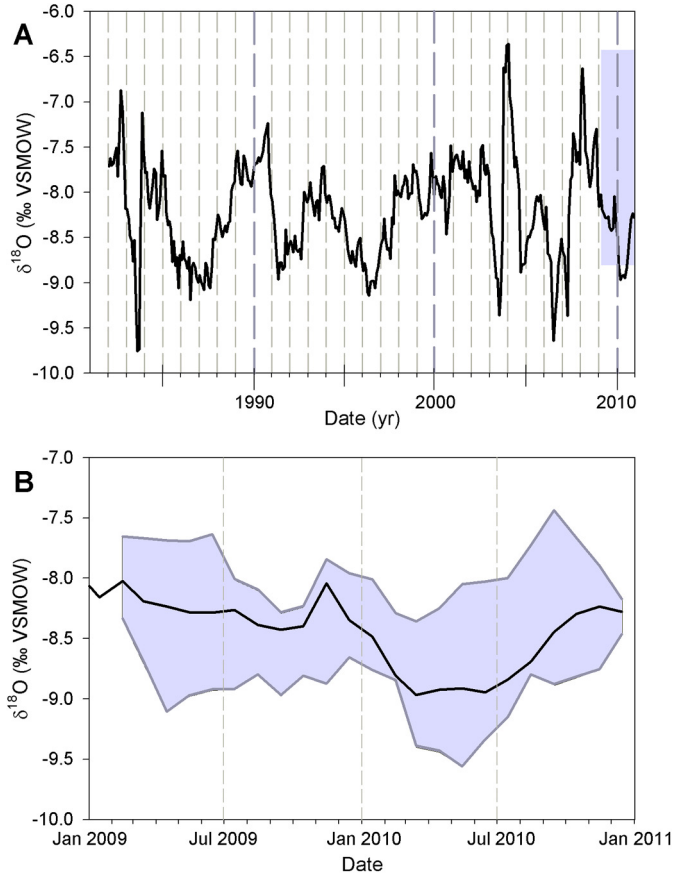

Fig. 8. Model of monthly $\delta^{18}O$ values of drip water in BiR hall using an infiltration mixing and transit time period of 11 months. A: Record of the modelled $\delta^{18}O$ values of drip water during the period 1982–2011. The grey box during the years 2009 and 2010 represent the period expanded in panel B. B: Comparison of $\delta^{18}O$ records of drip waters from the model and the monitoring period. The black line shows the model $\delta^{18}O$ signal of drip water during the years 2009 and 2010. The grey shaded area shows the range between the upper and lower limits of the 2 standard deviations of the monthly $\delta^{18}O$ values observed in the 9 drip sites, plotted from their average $\delta^{18}O$ values.

2 shows an exponential increase in discharge associated to precipitation events (Fig. 3). Most of the water discharged by this drip site outflows during these enhanced periods of drip rate, although our hydrological model confirmed that most of infiltrated water requires a delay of 11 months before dripping in BiR hall. Therefore, the quick response of drip rate to precipitation events results from a piston effect (Genty and Deflandre, 1998). Thus, the process of mixing in the karst aquifer filters out any potential seasonal component of dissolved organic matter in the infiltrated water, preventing the fluorescent laminae in PO2 to have seasonal periodicity. Instead, most likely these fluorescent laminae are related to the mixing of at least two reservoirs within the epikarst that have different average concentration of dissolved organic matter. The discharge dynamics recorded in drip site 2 is characteristic of drip sites fed by at least two reservoirs (Bradley et al., 2010). The first reservoir is responsible for the continuous drip rate at a base flow. The second reservoir provides a discontinuous discharge that supplies abundant amount of water only when the piston effect raises its water level causing overflow to the main conduits feeding the drip site. When the second reservoir supplies water to the drip site, the composition of the drip water experiences a mixing proportional to the amount of water supplied by each reservoir, and we observe transitional fluorescence patterns between end members. The reservoir triggering the exponential increase in drip rates does not necessarily involve shorter transit times of the infiltrated water in the aquifer, since its larger volume could compensate the discharge differences. Thus, the mixing period between most reservoirs in the aquifer may not differ significantly as supported by the homogeneous $\delta^{18}O$ variability recorded in different drip sites in BiR hall.

According to the average growth rate of PO2 stalagmite provided by the U–Th age model, we record in average at least 5 laminae per year (Fig. 3). During the monitoring period, the drip rate showed 7 or more events of increased drip rate per year. However, when these events occur in a short period of time, the drip rate does not decrease to the base flow and number of periods between high and base flow is reduced. During our survey at site 2, the number of recorded events and/or periods with high drip rate was similar to the average number of laminae expected to be recorded every year in the speleothem. Additionally, the mechanism previously described explains the different intensity of fluorescence observed in PO2 laminae. Therefore, the hydrological dynamics of drip site 2 supports that the laminae from PO2 stalagmite result from the mixing of at least two reservoirs within the aquifer above BiR hall and that their frequency is related to the events or periods of enhanced discharge which have a sub-annual frequency.

4.3. Other controls on the $\delta^{18}O$ record of PO2 stalagmite

Apart from the $\delta^{18}O$ values of drip water, the variability of the speleothem $\delta^{18}O$ record depends on the fractionation factor between the solution and the carbonate, and the existence of seasonal changes of growth rate. The water samples left to equilibrate with the moisture of the cave atmosphere did not have any measurable reduction of water volume and their isotope composition did not show signs of evaporation in the cave atmosphere. Therefore, we discard the existence of kinetic fractionation related to evaporation. However, fractionation of oxygen isotopes during the precipitation of calcite depends on temperature (Epstein et al., 1951). At common cave temperatures, these variations have to be larger than 0.4 or 0.5 °C, depending on the fractionation factor selected (Tremaine et al., 2011 and references therein), to reach the typical uncertainty in $\delta^{18}O$ analyses (i.e., 0.1‰). Previous studies in BiR hall showed that inter-annual and intra-annual thermal oscillations are <0.05 °C (Domínguez-Villar et al., 2015) and consequently, the temperature variability in the cave did not affect the $\delta^{18}O$ record of PO2 speleothem. Since drip water $\delta^{18}O$ values during the period of growth of PO2 speleothem were estimated instead of measured, we only can speculate whether the fractionation of oxygen isotopes between the solution and the calcite at the time of precipitation occurred under equilibrium conditions. However, the average $\delta^{18}O$ value of the top 500 μm of PO2 speleothem is within the range of the predicted isotope composition according to different fractionation factors (e.g., Tremaine et al., 2011) when using the constant temperature of 8.4 °C in BiR hall during last decades (Domínguez-Villar et al., 2015) and the average $\delta^{18}O$ value of modelled drip water. Therefore, it is reasonable to assume that PO2 speleothem precipitated under near-equilibrium conditions and that the speleothem $\delta^{18}O$ signal records the variability of the $\delta^{18}O$ values of drip water at the time of calcite precipitation.

On the other hand, a preferential seasonal growth rate can also determine the $\delta^{18}O$ value of analysed samples from the speleothem. This is not a problem when drip waters have a fairly stable $\delta^{18}O$ signal throughout the year (e.g., Boch et al., 2011). In our case, although the $\delta^{18}O$ values of drip waters do not have a distinctive seasonal component, they record significant variations during the year. This could potentially bias the $\delta^{18}O$ record of a speleothem having seasonal growth rate when compared to the average drip water $\delta^{18}O$ composition. Previous studies on drip sites from the same gallery showed that growth rate lacks seasonal-

ity and has a long-term trend resulting from inter-annual variability (Vokal, 1999; Genty et al., 2001). In the case of the PO2 speleothem, we do not discard that potential intra-annual growth rate variability of the PO2 speleothem could have introduced certain noise to the average speleothem $\delta^{18}O$ record when compared to the average drip water $\delta^{18}O$ values during the same period. However, we do not expect a systematic bias of the recorded speleothem $\delta^{18}O$ values due to the absence of a seasonal drip water $\delta^{18}O$ oscillation. The limited impact of the intra-seasonal variability of growth rate on the $\delta^{18}O$ values of the speleothem is supported by the coincidence within the uncertainties of the average composition of PO2 $\delta^{18}O$ record and the expected value of precipitated calcite from all the modelled drip water $\delta^{18}O$ values under equilibrium conditions.

4.4. Calibration of the $\delta^{18}O$ record of PO2 stalagmite

The radiocarbon analyses confirm that the top 500 µm of PO2 speleothem were formed at some point during the last 5 decades. The speleothem records three hiati in its topmost 1400 µm that supports discontinuous precipitation of calcite. However, there is no difference in the average thickness of laminae above or below the hiati (Table S3 in Supplementary Material). Therefore, the average growth rate is expected to be similar for the periods of calcite precipitation above and below the hiati. According to the age model based on U–Th dates, the PO2 speleothem has a narrow range of average growth rate (i.e., 15 to 40 µm/yr) during periods of continuous precipitation. Thus, considering that range of growth rate, the section of the speleothem between the hiati H2 and H1 (i.e., topmost 500 µm) could record 13 to 34 yr of speleothem growth.

The variability of the annual weighed $\delta^{18}O$ values of Ljubljana precipitation and the $\delta^{18}O$ record of the top of PO2 speleothem shows certain similarities (Fig. 6B and Fig. 7). Therefore, based on the available chronological evidence and the assumption that the variability of $\delta^{18}O$ of drip waters will be mostly captured by the speleothem, we assigned a tentative chronology to the top 500 µm of PO2 stalagmite. We do it by optimising the correlation coefficient between the modelled drip water $\delta^{18}O$ signal and the $\delta^{18}O$ record from PO2 speleothem. The data of modelled drip water $\delta^{18}O$ values considered a reference time period of 11 months, which is the mixing and transit time determined by our model in agreement with the monitoring data. The speleothem $\delta^{18}O$ values were integrated into portions of the speleothem that could have precipitated during periods of ~11 months. The best fit of data required integrating 1 to 3 analyses per period of 11 months and a single analysis was not assigned to more than one period. This integration of portions of the speleothem along the vertical axis of the sample could represent growth rates for individual periods of 11 months ranging from 14 to 50 µm, which is in good agreement with the average growth rate previously reported. The best fit between the speleothem $\delta^{18}O$ record and the modelled drip water $\delta^{18}O$ signal (Fig. 9) suggests that the topmost 500 µm of the speleothem precipitated during 19 yr (i.e., 21 periods of 11 months) between the years 1984 and 2003 ($r^2 = 0.64$; p-value <0.001). According to this tentative age model, the average growth rate of this portion of the speleothem was 27 µm/yr, which is exactly the same average growth rate that we calculated below the H3 hiatus.

The tentative age model produces a good correlation between the $\delta^{18}O$ records of the modelled drip water and the speleothem. However, is this correlation the result of two synchronous records with a causal relationship, or could be a casual correlation of two independent time series? We produced one million virtual speleothem $\delta^{18}O$ records and compared them to the modelled drip water $\delta^{18}O$ signal between the years 1984 and 2003. The virtual

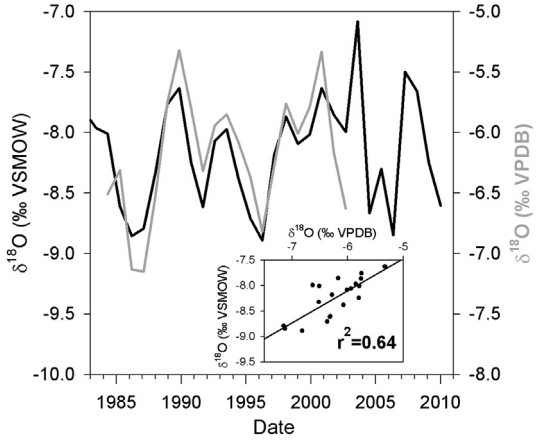

Fig. 9. Comparison of the record of modelled drip water $\delta^{18}O$ values in BiR hall weighed for periods of 11 months from the year 1983 until 2011 and the record of $\delta^{18}O$ values of PO2 speleothem using a tentative age model that optimises the correlation of the data. See text for further details.

speleothem records were produced randomly within the variability (i.e., 2 SD) of the $\delta^{18}O$ values of the modelled drip water between 1984 and 2003. Only one in 20.000 virtual $\delta^{18}O$ records have correlations with PO2 $\delta^{18}O$ record as good as the one here reported. Considering that the top 500 µm of PO2 speleothem were formed during the past five decades, we have only 30 combinatory options to allocate 21 periods of 11 months. Therefore, the good correlation found between model and PO2 $\delta^{18}O$ records is highly unlikely to be casual (i.e., probability = 0.0015). Therefore, we can confirm the tentative age model for the topmost 500 µm of PO2 speleothem. This calibration test shows that the $\delta^{18}O$ record of PO2 speleothem accurately records the isotope composition of precipitation over the region filtered through the epikarst.

5. Conclusions

We used an ion microprobe to analyse the $\delta^{18}O$ record of a slow growth rate speleothem precipitated until recent times in Postojna Cave. The speleothem was not actively forming at the time of collection, although U–Th dates support its growth until recent times. Fluorescent laminae in the speleothem had sub-annual frequency and could not be used to establish an annually resolved chronology. On the other hand, we modelled the $\delta^{18}O$ composition of drip water in the studied cave, using a regional $\delta^{18}O$ record of precipitation with monthly resolution. The model was validated using water $\delta^{18}O$ composition of several drip sites measured during a two-year monitoring period. The results suggest that water had a transit and mixing time of 11 months after its infiltration in the aquifer. The comparison of the speleothem $\delta^{18}O$ record with the modelled $\delta^{18}O$ composition of drip water confirmed that the speleothem precipitated during the years 1984 and 2003. The annually resolved age model during this period was based on the best correlation of these two records supported by ^{14}C and U–Th data. We also conclude that the $\delta^{18}O$ signal of the speleothem records the inter-annual variability of the regional $\delta^{18}O$ composition of precipitation without any seasonal bias, and that the hydrological dynamics recorded during the monitoring period are stationary at decadal timescale.

This research shows the potential of ion microprobe analyses to perform calibration tests on recent speleothems with slow growth rates. Additionally, we demonstrated that calibration tests at annual resolution are still possible in samples not actively growing at the time of collection. We have also shown that under certain circumstances it is possible to achieve annually resolved speleothem chronologies from speleothems lacking annual laminae.

Acknowledgements

We thank Postojnska jama d.d. and the Ministry of Environment and Spatial Planning of Slovenia for the permissions to access the cave and to sample the speleothem. We appreciate the support of Stanislav Glažar, who joined us in every visit to the cave during the monitoring period. We are grateful to Andrej Mihevc from the Karst Research Institute in Postojna who supervised the speleothem collection in the cave. Ion probe analyses were conducted in WiscSIMS laboratory at the University of Wisconsin-Madison thanks to the essential support and advice of John W. Valley. We thank Ian J. Orland and Kathleen A. Wendt for their discussion and support in the analytical design and the fluorescence imaging of PO2 stalagmite. We thank Stojan Žigon for water stable isotope analyses at Jožef Stefan. Radiocarbon analyses were supported by the NERC radiocarbon facility (allocation number 1404.0409) thanks to the collaboration of Andy Baker. One of the authors (SL) received funds from the Slovenian Research Agency (research programme P1-0143 and and project N1-0054) the EU Horizon 2020 project MASSTWIN (grant agreement No. 692241).

Appendix A. Supplementary material

Supplementary material related to this article can be found online at https://doi.org/10.1016/j.epsl.2017.11.012.

References

Ayalon, A., Bar-Matthews, M., Sass, E., 1998. Rainfall-recharge relationships within a karstic terrain in the Eastern Mediterranean semi-arid region, Israel: $\delta^{18}O$ and δD characteristics. J. Hydrol. 207, 18–31.

Baker, A., Barnes, W.L., Smart, P.L., 1996. Speleothem luminescence intensity and spectral characteristics: signal calibration and record of palaeovegetation. Chem. Geol. 130, 65–76.

Baker, A., Wilson, R., Fairchild, I.J., Franke, J., Spötl, C., Mattey, D., Trouet, V., Fuller, L., 2011. High resolution $\delta^{18}O$ and $\delta^{13}C$ records from an annually laminated Scottish stalagmite and relationship with last millennium climate. Glob. Planet. Change 79, 303–311.

Baker, A., Bradley, C., Phipps, S.J., Fischer, M., Fairchild, I.J., Fuller, L., Spötl, C., Azcurra, C., 2012. Millennial-length forward models and pseudoproxies of stalagmite $\delta^{18}O$: an example from NW Scotland. Clim. Past 8, 1153–1167.

Ban, F., Pan, G., Wang, X., 2005. Timing and possible mechanism of organic substance formation in stalagmite laminae from Beijing Shihua Cave. Quat. Sci. 25, 265–268 (in Chinese).

Boch, R., Spötl, C., Frisia, S., 2011. Origin and palaeoenvironmental significance of lamination in stalagmites from Katerloch Cave, Austria. Sedimentology 58, 508–531.

Bradley, C., Baker, A., Jex, C.N., Leng, M.J., 2010. Hydrological uncertainties in the modelling of cave drip-water $\delta^{18}O$ and the implications for stalagmite palaeoclimate reconstructions. Quat. Sci. Rev. 29, 2201–2214.

Brenčič, M., Kononova, N.K., Vreča, P., 2015. Relation between isotopic composition of precipitation and atmospheric circulation patterns. J. Hydrol. 529, 1422–1432.

Burns, S.J., Fleitmann, D., Mudelsee, M., Neff, U., Matter, A., Mangini, A., 2002. A 780-year annually resolved record of Indian Ocean monsoon precipitation from a speleothem from south Oman. J. Geophys. Res. 107 (D20), 4434.

Cheng, H., Edwards, R.L., Shen, C.C., Polyak, V.J., Asmerom, Y., Woodhead, J., Hellstrom, J., Wang, Y., Kong, X., Spötl, C., Wang, X., Alexander, E.C., 2013. Improvements in ^{230}Th dating, ^{230}Th and ^{234}U half-life values, and U–Th isotopic measurements by multi-collector inductively coupled plasma mass spectrometry. Earth Planet. Sci. Lett. 371–372, 82–91.

Domínguez-Villar, D., Fairchild, I.J., Baker, A., Carrasco, R.M., Pedraza, J., 2013. Reconstruction of cave air temperature based on surface atmosphere temperature and vegetation changes: implications for speleothem paleoclimate records. Earth Planet. Sci. Lett. 369–370, 158–168.

Domínguez-Villar, D., Lojen, S., Krklec, K., Baker, A., Fairchild, I.J., 2015. Is global warming affecting cave temperature? Experimental and model data from a paradigmatic case study. Clim. Dyn. 45, 569–581.

Domínguez-Villar, D., Wang, X., Krklec, K., Cheng, H., Edwards, R.L., 2017. The control of the tropical North Atlantic on Holocene millennial climate oscillations. Geology 45, 303–306.

Dorale, J.A., Edwards, R.L., Alexander Jr., E.C., Shen, C.C., Richards, D.A., 2004. Uranium series dating of speleothems: current techniques, limits & applications. In: Sasowsky, I.D., Mylroie, J.E. (Eds.), Studies of Cave Sediments. Kluwer Academic/Plenum Publishers, New York, pp. 177–198.

Edwards, R.L., Chen, J.H., Wasserburg, G.J., 1986. ^{238}U–^{234}U–^{230}Th–^{232}Th systematics and the precise measurements of time over the past 500,000 years. Earth Planet. Sci. Lett. 81, 175–192.

Epstein, S., Buchsbaum, R., Lowenstam, H., Urey, H.C., 1951. Carbonate-water isotopic temperature scale. Geol. Soc. Am. Bull. 62, 417–426.

Epstein, S., Mayeda, T., 1953. Variation of O^{18} content of waters from natural sources. Geochim. Cosmochim. Acta 4, 213–224.

Fairchild, I.J., Baker, A., 2012. Speleothem Science: From Processes to Past Environments. Wiley–Blackwell, Chichester.

Feng, W., Casteel, R.C., Banner, J., Heinze-Fry, A., 2014. Oxygen isotope variations in rainfall, drip water and speleothem calcite from a well-ventilated cave in Texas, USA: assessing a new speleothem temperature proxy. Geochim. Cosmochim. Acta 127, 233–250.

Fischer, M.J., Treble, P.C., 2008. Calibrating climate-$\delta^{18}O$ regression models for the interpretation of high-resolution speleothem $\delta^{18}O$ time series. J. Geophys. Res. 113, D17103.

Genty, D., Deflandre, G., 1998. Drip flow variations under a stalactite of the Père Noel cave (Belgium). J. Hydrol. 211, 208–232.

Genty, D., Massault, M., 1999. Carbon transfer dynamics from bomb-^{14}C and $\delta^{13}C$ time series of a laminated stalagmite from SW France – modelling and comparison with other stalagmite records. Geochim. Cosmochim. Acta 63, 1537–1548.

Genty, D., Vokal, B., Obelic, B., Massault, M., 1998. Bomb ^{14}C time history recorded in two modern stalagmites – importance for soil organic dynamics and bomb ^{14}C distribution over continents. Earth Planet. Sci. Lett. 160, 795–809.

Genty, D., Baker, A., Vokal, B., 2001. Intra- and inter-annual growth rate of modern stalagmites. Chem. Geol. 176, 191–212.

IAEA/WMO, 2009. Global network of isotopes in precipitation. The GNIP database. Accessible at: http://www.iaea.org/water.

Jex, C.N., Baker, A., Leng, M.J., Sloane, H.J., Eastwood, W.J., Fairchild, I.J., Thomas, L., Bekaroglu, E., 2010. Calibration of speleothem $\delta^{18}O$ with instrumental climate records from Turkey. Glob. Planet. Change 71, 207–217.

Kita, N.T., Ushikubo, T., Fu, B., Valley, J.W., 2009. High precision SIMS oxygen isotope analysis and the effect of simple topography. Chem. Geol. 264, 43–57.

Kolodny, Y., Bar-Matthews, M., Ayalon, A., McKeegan, K.D., 2003. A high spatial resolution $\delta^{18}O$ profile of a speleothem using an ion-microprobe. Chem. Geol. 197, 21–28.

Kozdon, R., Ushikubo, T., Kita, N.T., Spicuzza, M., Valley, J.W., 2009. Intratest oxygen isotope variability in the planktonic foraminifer N. pachyderma: real vs. apparent vital effects by ion microprobe. Chem. Geol. 258, 327–337.

Kranjnc, B., Ferlan, M., Ogrinc, N., 2017. Soil CO_2 sources above a subterranean cave—Pisani rov (Postojna Cave, Slovenia. J. Soil Sediments 17, 1883–1892.

Krklec, K., Domínguez-Villar, D., Lojen, S., 2016. Moisture sources of precipitation over Postojna (Slovenia) and implication of its isotope composition. Geophys. Res. Abstr. 18, EGU2016–EGU3910.

Lauritzen, S.E., Lunberg, J., 1999. Calibration of the speleothem delta function: an absolute temperature record for the Holocene in northern Norway. Holocene 9, 659–669.

Liu, Y.H., Tang, G.Q., Ling, X.X., Hu, C.Y., Li, X.H., 2015. Speleothem annual layers revealed by seasonal SIMS $\delta^{18}O$ measurements. Sci. China Earth Sci. 58, 1741–1747.

Markowska, M., Baker, A., Andersen, M.S., Jex, C.N., Cuthbert, M.O., Rau, G.C., Graham, P.W., Rutlidge, H., Mariethoz, G., Marjo, C.E., Treble, P.C., Edwards, N., 2016. Semi-arid zone caves: evaporation and hydrological controls on $\delta^{18}O$ drip water composition and implications for speleothem paleoclimate reconstructions. Quat. Sci. Rev. 131, 285–301.

Mattey, D., Lowry, D., Duffet, J., Fisher, R., Hodge, E., Frisia, S., 2008. A 53 year seasonally resolved oxygen and carbon isotope record from a modern Gibraltar speleothem: reconstructed drip water and relationship to local precipitation. Earth Planet. Sci. Lett. 269, 80–95.

Orland, I.J., Bar-Matthews, M., Kita, N.T., Ayalon, A., Matthews, A., Valley, J.W., 2009. Climate deterioration in the Eastern Mediterranean as revealed by ion microprobe analyses of a speleothem that grew from 2.2 to 0.9 ka in Soreq Cave, Israel. Quat. Res. 71, 27–35.

Orland, I.J., Bar-Matthews, M., Ayalon, A., Matthews, A., Kozdon, R., Ushikubu, T., Valley, J.W., 2012. Seasonal resolution of Eastern Mediterranean climate change since 34 ka from Soreq Cave speleothem. Geochim. Cosmochim. Acta 89, 240–255.

Orland, I.J., Burstyn, Y., Bar-Matthews, M., Kozdon, R., Ayalon, A., Matthews, A., Valley, J.W., 2014. Seasonal climate signals (1990–2008) in a modern Soreq Cave stalagmite as revealed by high-resolution geochemical analyses. Chem. Geol. 363, 322–333.

Orland, I.J., Edwards, R.L., Cheng, H., Kozdon, R., Cross, M., Valley, J.W., 2015. Direct measurements of deglacial monsoon strength in a Chinese stalagmite. Geology 43, 555–558.

Pacton, M., Breitenbach, S.F.M., Lechleitner, F.A., Vaks, A., Rollion-Bard, C., Gutareva, O.S., Osintcev, A.V., Vasconcellos, C., 2013. The role of microorganisms in the formation of a stalactite in Botovskaya Cave, Siberia – paleoenvironmental implications. Biogeosciences 10, 6115–6130.

Ramsey, C.B., 2008. Deposition models for chronological records. Quat. Sci. Rev. 27, 42–60.

Riechelmann, S., Schröder-Ritzrau, A., Spötl, C., Riechelmann, D.F.C., Richter, D.K., Mangini, A., Frank, R., Breitenbach, S.F.M., Immenhauser, A., 2017. Sensitivity of Bunker Cave to climatic forcings highlighted through multi-annual monitoring of rain-, soil-, and dripwaters. Chem. Geol. 449, 194–205.

Spötl, C., Mattey, D., 2006. Stable isotope microsampling of speleothems for palaeoenvironmental studies: a comparison of microdrill, micromill and laser ablation techniques. Chem. Geol. 235, 48–58.

Treble, P.C., Chappell, J., Gagan, M.K., McKeegan, K.D., Harrison, T.M., 2005. In situ measurements of seasonal $\delta^{18}O$ variations and analysis of isotopic trends in a modern speleothem from southwest Australia. Earth Planet. Sci. Lett. 233, 17–32.

Treble, P.C., Schmidt, A.K., Edwards, R.L., McKeegan, K.D., Harrison, T.M., Grove, M., Cheng, H., Wang, Y.J., 2007. High resolution Secondary Ionization Mass Spectrometry (SIMS) $\delta^{18}O$ analyses of Hulu Cave speleothem at the time of Heinrich Event 1. Chem. Geol. 238, 197–212.

Tremaine, D.M., Froelich, P.N., Wang, Y., 2011. Speleothem calcite farmed in situ: modern calibration of $\delta^{18}O$ and $\delta^{13}C$ paleoclimate proxies in a continuously-monitored natural cave system. Geochim. Cosmochim. Acta 75, 4929–4950.

Valley, J.W., Kita, N.T., 2005. First results from UW CAMECA IMS-1280. In: Fourth Biennial Geochemical SIMS Workshop.

Vokal, B., 1999. The Carbon Transfer in Karst Areas – An Application to the Study of Environmental Changes and Paleoclimatic Reconstruction. Ph.D. thesis. School of Environmental Sciences, Polytechnic Nova Gorica, Slovenia.

Vreča, P., Krajcar Bronić, I., Horvatinčić, N., Barešić, J., 2006. Isotopic characteristics of precipitation in Slovenia and Croatia: comparison of continental and marine stations. J. Hydrol. 330, 457–469.

Wang, Y., Cheng, H., Edwards, R.L., An, Z., Wu, J., Shen, C.C., Dorale, J.A., 2001. Absolute-dated Late Pleistocene monsoon record from Hulu Cave, China. Science 294, 2345–2348.

Yudava, M.G., Ramesh, R., Pant, G.B., 2004. Past monsoon rainfall variations in Peninsular India recorded in a 331-year old speleothem. Holocene 14, 517–524.